Applied Energy 111 (2013) 1001–1009

Contents lists available at SciVerse ScienceDirect

Applied Energy

journal homepage: www.elsevier.com/locate/apenergy

Energy efficiency analysis of a series plug-in hybrid electric bus with different energy management strategies and battery sizes

Xiaosong Hu *, Nikolce Murgovski, Lars Johannesson, Bo Egardt

Department of Signals and Systems, Chalmers University of Technology, 41296 Gothenburg, Sweden

HIGHLIGHTS

- Recuperation and fuel-to-traction efficiencies are analyzed for a PHEV powertrain.
- Two different energy controls are compared in terms of the two efficiencies.
- Impact of battery downsizing on the two efficiencies is quantified.
- Convex modeling and optimization are used to analyze the powertrain.

ARTICLE INFO

Article history:
Received 8 February 2013
Received in revised form 15 May 2013
Accepted 29 June 2013
Available online 22 July 2013

Keywords:
Recuperation efficiency
Fuel-to-traction efficiency
TTW analysis
Plug-in hybrid electric vehicle
Convex optimization

ABSTRACT

This paper is concerned with the tank-to-wheel (TTW) analysis of a series plug-in hybrid electric bus operated in Gothenburg, Sweden. The bus line and the powertrain model are described. The definition and the calculation method of the recuperation and fuel-to-traction efficiencies are delineated for evaluating the TTW energy conversion. The two efficiencies are quantified and compared for two optimization-based energy management strategies, in which convex modeling and optimization are used. The impact of downsizing the battery on the two efficiencies is also investigated.

1. Introduction

Oil supply uncertainty, growing mobility demand, and increasingly stringent regulations on pollutants and carbon footprint are expediting a paradigm shift towards sustainable transportation [1–3]. As key ingredients, hybrid electric vehicles (HEVs) are being actively developed by automotive companies worldwide to pursue higher fuel economy than conventional internal-combustion-engine (ICE) vehicles without inducing range anxiety [4–8]. Owing to vehicle-to-grid (V2G) services, plug-in hybrid electric vehicles (PHEVs) potentially can take advantage of renewable energy sources to reduce reliance on fossil fuels and thus are an important solution to reducing carbon dioxide emission in the transportation sector [9,10].

In order to evaluate the total energy consumption and carbon dioxide emission of a vehicle in a broad sense, well-to-wheel (WTW) analysis is often needed [11–14]. It consists of well-to-tank (WTT) and tank-to-wheel (TTW) analyses. WTT takes the upstream processes into account and focuses on the fuel production, processing, and delivery, such as oil refinery and electricity generation, in which sophisticated chemical and physical processes are involved. TTW is concerned with energy conversion efficiency from the on-board fuel/electricity to the mechanical energy demanded at the wheels. For automotive engineers, TTW is often applied to assess the energy-saving capability of a vehicle design and to guide the improvement of the vehicle energy efficiency. In this study, the TTW energy analysis is therefore considered.

One lumped energy efficiency-a ratio of the demanded mechanical energy at the wheels to the needed fuel energy-was commonly used for the TTW analysis of a vehicle [12,13,15]. This lumped TTW efficiency is well suited for conventional ICE vehicles. Nevertheless, for HEVs or PHEVs with braking energy regeneration, the efficiency may become arbitrarily large, leading to no significance [16].

Another method to describe the TTW analysis of electrified mobility is to characterize each energy conversion process occurring inside the driveline by an averaged efficiency over the driving cycle. For example, energy conversion efficiencies of hybrid electric vehicles with different topologies were investigated by using this

* Corresponding author. Address: E-building, Hörsalsvägen 11, 41296 Gothenburg, Sweden. Tel.: +46 31 772 1538; fax: +46 31 772 1748.
E-mail address: xiaosong@chalmers.se (X. Hu).

0306-2619/$ - see front matter © 2013 Elsevier Ltd. All rights reserved.
http://dx.doi.org/10.1016/j.apenergy.2013.06.056

methodology [17–20]. The energy conversion phenomena in PHEVs were also analyzed by considering the complete energy path [21]. The advantage of the approach is the availability of a thorough understanding of efficiencies of all the energy conversion steps within the powertrain. However, since the method needs a plethora of distinct efficiencies, the large complexity may be undesirable to a system-level fuel/electricity energy estimation and analysis for HEVs or PHEVs.

Recently, a simple yet useful concept for the TTW analysis was proposed for HEVs [16]. In order to account for the energy recuperation, the mechanical energy demand at the wheels is viewed as a summation of dissipative energy and circulating energy. Accordingly, the fuel-to-traction efficiency and recuperation efficiency are defined to evaluate the TTW process, rather than one lumped efficiency. The novel concept is the most simple and straightforward extension of the conventional TTW efficiency, which is meaningful and applicable to vehicles with energy recuperation. Furthermore, it allows automotive engineers to easily assess the energy effectiveness of electrified powertrains and to find possible solutions with enhanced energy efficiencies from a system level.

The fuel-to-traction and recuperation efficiencies of a parallel hybrid electric passenger car with an optimal control strategy were analyzed in [16]. However, in the literature, there is a lack of discussion on quantification of the two efficiencies for PHEVs, particularly on how PHEV energy management strategy and battery size influence them. The purpose of this paper is to analyze the fuel-to-traction and recuperation efficiencies for a series plug-in hybrid electric bus operating in Gothenburg, Sweden. The main contribution is twofold: (1) the fuel-to-traction and recuperation efficiencies of the bus are analyzed and compared for two different optimization-based energy management strategies, i.e., the charge-depleting and charge-sustaining (CD–CS) and blended controls [22–27]. The convex optimization is herein adopted for the two strategies, as it has been certified in our previous work [28–30] that compared to dynamic programming (a benchmark), the convex optimization can accomplish a comparable result with a much lower computational intensity; (2) how downsizing the bus battery affects the two efficiencies is quantified.

The remainder of the paper is organized as follows: Section 2 introduces the bus line and the powertrain model; the definition and the calculation method of the fuel-to-traction and recuperation efficiencies are depicted in Section 3; the convex optimization-based two energy management strategies for the bus are presented in Section 4; the energy efficiency analysis and comparison for the two strategies are discussed in Section 5, in which the impact of downsizing the battery on the bus energy efficiencies is evaluated; Conclusions are finally drawn in Section 6.

2. Bus line and powertrain model

The PHEV considered in this study is a bus with a series powertrain topology [28]. The powertrain does not have a direct mechanical link between the ICE and the wheels, as shown in Fig. 1. The wheels are propelled by a 220 kW electrical motor (EM, 2200 rpm, and no EM reduction gear) powered by a lithium-ion battery pack and/or a 180 kW engine-generator unit (EGU). The bus is driven on a bus line in Gothenburg, Sweden, which is described by demanded velocity and road gradient at each point of time (see Fig. 2). The quasi-static modeling methodology is employed to model the powertrain [5]. The velocity and force demands of the bus can be translated into an angular velocity $\omega(t)$ and torque $T_v(t)$ on the shaft between the EM and the final drive, given the demanded acceleration and speed on the bus line and the known vehicle parameters, such as inertia, aerodynamic drag, rolling resistance, and wheel radius.

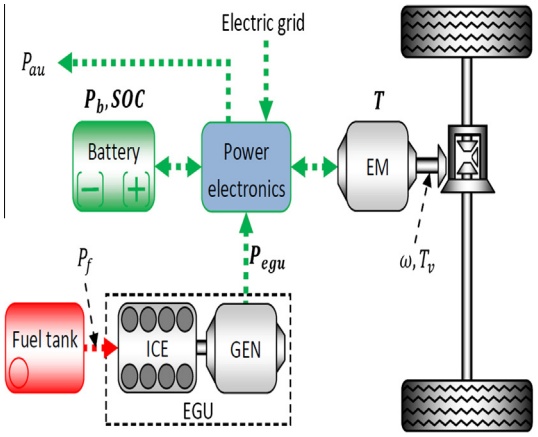

Fig. 1. Powertrain configuration of the plug-in bus.

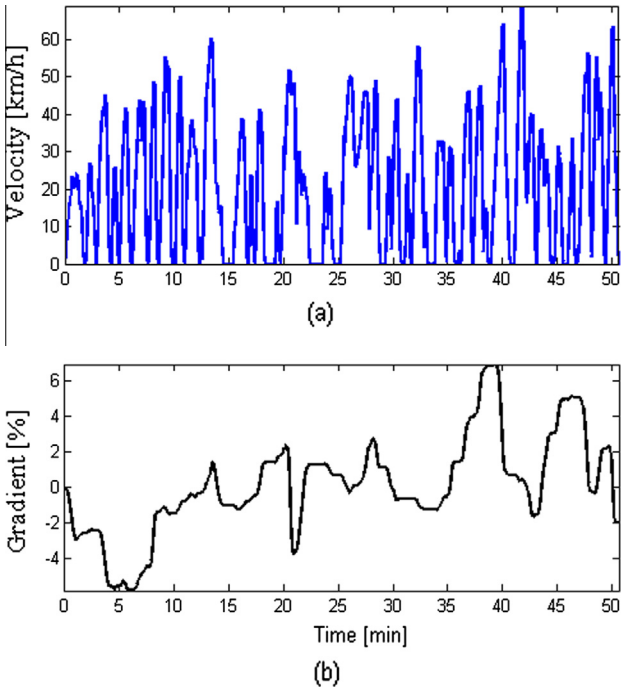

Fig. 2. Driving cycle of the bus line: (a) velocity demand; (b) road gradient.

The EM, which delivers a torque $T(t)$, is designed to be able to meet the high torque demands. Moreover, the EM is also used to recuperate braking energy; when either its torque limit $T_{min}(\omega(t))$ or the battery charging limit is met, friction braking is supplemented. The power balance equation is described as

$$P_m(t) + P_{loss,m}(t) + P_{au}(t) = \boldsymbol{P_b}(t)\eta_1 + \boldsymbol{P_{egu}}(t)\eta_{con}, \quad (1)$$

where P_m is the EM power on the shaft between the EM and the final drive calculated by

$$P_m(t) = \boldsymbol{T}(t)\omega(t), \quad (2)$$

and $P_{loss,m}$ is the EM power loss characterized by a quadratic function of the motor torque

$$P_{loss,m} = b_0(\omega)\boldsymbol{T^2} + b_1(\omega)\boldsymbol{T} + b_2(\omega), \quad (3)$$

in which b_0, b_1, and b_2 are nonnegative speed-dependent coefficients. P_{au}, $\boldsymbol{P_b}$, and $\boldsymbol{P_{egu}}$ are the auxiliary power, battery power, and EGU power, respectively. η_{con} is the efficiency of the power con-

verter (here the averaged efficiency is used, since our focus is on the system-level behavior of the powertrain [5,28]), and

$$\begin{cases} \eta_1 = \eta_{con}, & \boldsymbol{P_b} \geq 0 \\ \eta_1 = \frac{1}{\eta_{con}}, & \boldsymbol{P_b} < 0. \end{cases} \tag{4}$$

In order to preserve the optimization problem convexity (described later in Section 4), Eq. (1) can be rewritten as

$$P_m(t) + P_{loss,m}(t) + P_{au}(t) = \min\left(\boldsymbol{P_b}(t)\eta_{con}, \frac{\boldsymbol{P_b}(t)}{\eta_{con}}\right) + \boldsymbol{P_{egu}}(t)\eta_{con}. \tag{5}$$

The EGU power loss is modeled as a quadratic function of P_{egu}, thereby yielding the fossil fuel (diesel) power

$$P_f(t) = a_0\boldsymbol{P}^2_{\boldsymbol{egu}}(t) + (a_1+1)\boldsymbol{P_{egu}}(t) + a_2 e(t) \tag{6}$$

with $a_i \geqslant 0$, $i \in \{0,2\}$. For better readability, we represent all the optimization variables in bold. The binary signal $e(t)$ allows for zero diesel power by removing the idling loss a_2 when the engine is off. $e(t)$ is herein determined by heuristics that turn the engine on if the vehicle power exceeds a threshold P^*_{on}, i.e.,

$$e(t) = \begin{cases} 1, & T_v(t)\omega(t) \geq P^*_{on} \\ 0, & \text{otherwise}. \end{cases} \tag{7}$$

The optimal power threshold P^*_{on} is found by iteratively solving the convex optimization problem for several values of P_{on} within the power range of the vehicle. The detailed procedure can be found in [29], where it has been shown that these heuristics ensure a solution close to the global optimum. The efficiencies of the EM and EGU are illustrated in Fig. 3. The quadratic efficiency functions, i.e., Eqs. (3) and (6), are used to preserve the optimization problem convexity, and details on the validity of using quadratic losses for these components can be found in [29–31].The battery pack consists of n_c consistent cells, where each cell is modeled as a simple resistive circuit. Therefore, the pack power can be described by

$$\boldsymbol{P_b}(t) = (V_{oc}(t)I(t) - I^2(t)R)n_c, \tag{8}$$

where V_{oc} is the cell open circuit voltage (OCV), I is the cell current, and R is the internal resistance (assumed constant). According to Eq. (8), the current I can be expressed as

$$I(t) = \frac{1}{2R}\left(V_{oc}(t) - \sqrt{V^2_{oc}(t) - \frac{4R\boldsymbol{P_b}(t)}{n_c}}\right) \in [I_{min}, I_{max}], \tag{9}$$

where $[I_{min}, I_{max}]$ is the cell current limits. Additionally, the pack power is limited by

$$\boldsymbol{P_b}(t) \leq \frac{V^2_{oc}(t)n_c}{4R}. \tag{10}$$

The cell OCV $V_{oc}(t)$ is modeled as an affine function of State-of-Charge (SOC)

$$V_{oc}(t) = d_0\boldsymbol{SOC}(t) + d_1, \tag{11}$$

which is a rational approximation within the cell SOC range $[SOC_{min}, SOC_{max}]$ in PHEVs applications, especially for lithium iron phosphate cells, such as A123's ANR26650m1 cell (see Fig. 4). The cell dynamics is described by

$$\frac{d\boldsymbol{SOC}(t)}{dt} = -\frac{I(t)}{Q_n}, \tag{12}$$

where Q_n is the cell nominal capacity. A constraint is imposed on the initial SOC

$$\boldsymbol{SOC}(t_0) = SOC_0. \tag{13}$$

The main specification of the cell (A123's ANR26650m1) is listed in Table 1, where the internal resistance is an average in the usable SOC range [29,31,40]. Cell packaging and circuitry are assumed to account for 12.3% of the total mass of the battery pack [32]. The main vehicle parameters are shown in Table 2. For simplicity, we assume that there is the constant number of passengers on board. Note that since the bus operates on a specific route and experiences a relatively long-time downward slope (see Fig. 2) at the beginning, the battery initial SOC is specified to be 60% rather than 80% to be able to recuperate the initial braking energy.

3. Fuel-to-traction and recuperation efficiencies for plug-in bus

3.1. Dissipative energy and circulating energy

The traction power $P(t)$ that is used to propel the wheels and auxiliary devices of the bus is calculated by

$$P(t) = P_{ae}(t) + P_{rol}(t) + P_{au}(t) + P_{ac}(t) + P_{gr}(t), \tag{14}$$

where $P_{ae}(t) = \rho_{air}A_f c_d v^3(t)/2$ is the power to overcome the aerodynamic drag force, with v being the vehicle velocity; $P_{rol}(t) = (m_v + m_p)gc_r\cos(\alpha(t))v(t)$ is the power to overcome the rolling resistance, in which α is the slope, and m_p is the pack mass; $P_{ac}(t) = (m_v + m_p)v(t)\frac{dv(t)}{dt}$ and $P_{gr}(t) = (m_v + m_p)g\sin(\alpha(t))v(t)$ are

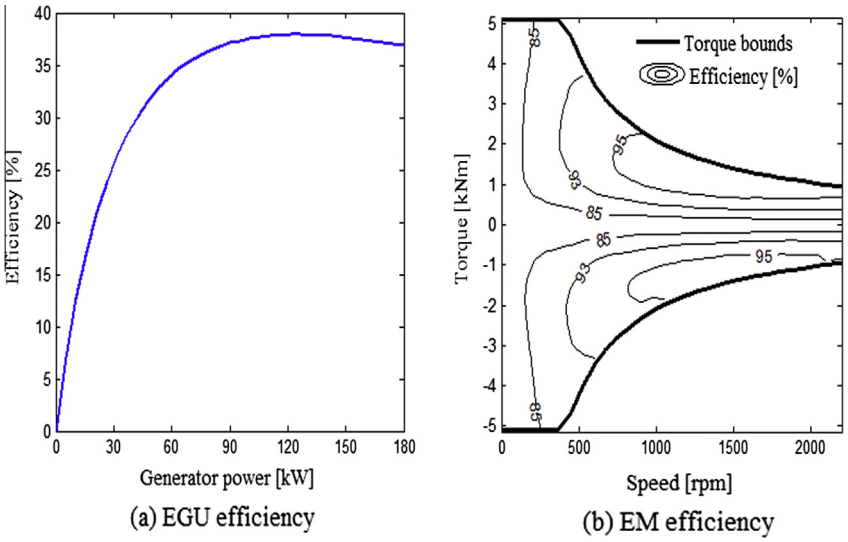

Fig. 3. Efficiencies of the EGU and EM: (a) EGU; (b) EM.

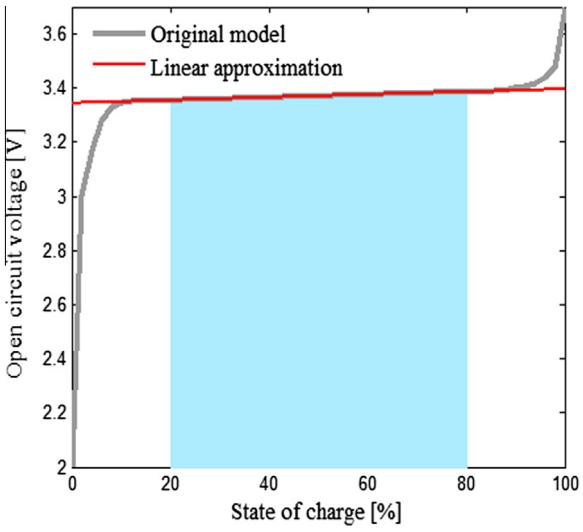

Fig. 4. Cell OCV approximation (A123's ANR26650m1 cell).

Table 1
Li-ion cell specification.

Nominal capacity	Q_n = 8280 As
Nominal voltage	$\overline{V}_{oc}$ = 3.3V
Maximum discharging current	I_{max} = 70 A
Maximum charging current	I_{min} = −45 A
Internal resistance	R = 0.01 Ω
Mass	m_{bc} = 0.07 kg
Coefficient for OCV approximation	d_0 = 0.5 V
Coefficient for OCV approximation	d_1 = 2.95 V

Table 2
Vehicle parameters.

Parameter	Value	Parameter	Value
Frontal area	A_f = 7.54 m^2	Averaged converter efficiency	η_{con} = 98%
Aerodynamic drag coefficient	c_d = 0.7	Final drive efficiency	η_{fd} = 97%
Air density	ρ_{air} = 1.184 kg/m^3	Diesel price	c_f = 3.47 × 10^{-8} €/J
Gravity	g = 9.81 m/s^2	Electricity price	c_{el} = 2.78 × 10^{-8} €/J
Rolling resistance coefficient	c_r = 0.007	Minimum allowable pack SOC	SOC_{min} = 20%
Wheel radius	R_w = 0.509 m	Maximum allowable pack SOC	SOC_{max} = 80%
Final gear	γ = 4.7	Initial SOC	SOC_0 = 60%
Vehicle Mass excluding the pack	m_v = 14.5 ton	Base number of cells	n_c = 1000

the powers for acceleration/deceleration and driving uphill/downhill, respectively. $P(t)$ can be split up into two groups: one is the dissipative power $P_{dis}(t) = P_{ae}(t) + P_{rol}(t) + P_{au}(t)$; the other is the conservative power $P_{cons}(t) = P_{ac}(t) + P_{gr}(t)$ [16]. Since the initial velocity and altitude of the bus are the same as those at the final time in the driving cycle, the integration of the conservative power over the duration of the cycle is equal to zero. If there is a perfect recuperation, the traction energy demand per distance E_{trac} would equal the dissipative energy E_{dis} per distance

$$E_{trac} = \frac{\int_{t_0}^{t_f} P(t)dt}{d} = \frac{\int_{t_0}^{t_f} P_{dis}(t)dt}{d} = E_{dis}, \tag{15}$$

where t_0, t_f, and d are the initial time, final time, and the driving distance in the cycle, respectively. If there is no recuperation (i.e., ICE vehicles),

$$E_{trac} = \frac{\int_{P(t)\geq 0} P(t)dt}{d} = \frac{\int_{t_0}^{t_f} P_{diss}(t)dt}{d} + \frac{\int_{P(t)<0} -P(t)dt}{d} = E_{dis} + \frac{\int_{P(t)<0} -P(t)dt}{d}, \tag{16}$$

where the term $\frac{\int_{P(t)<0} -P(t)dt}{d}$ is the circulating energy per distance E_{cir} that is a temporal vehicle energy circulating in the form of kinetic or potential energy and is ultimately dissipated during friction braking. Therefore, Eq. (16) for vehicles without recuperation functionality can be abbreviated as

$$E_{trac} = E_{dis} + E_{cir}. \tag{17}$$

In the case of a real recuperation, the following energy balance equation holds

$$E_{trac} = E_{dis} + E_{cir} - E_{rec}, \tag{18}$$

where E_{rec} is the net energy recuperated that is usable for traction. According to Eqs. (15) and (18), it can be found that the perfect recuperation is $E_{rec} = E_{cir}$.

3.2. Recuperation efficiency

The recuperation efficiency is defined as follows:

$$\eta_{rec} = \frac{E_{rec}}{E_{cir}}. \tag{19}$$

Since E_{cir} can be easily achieved from the driving cycle, the key task is to calculate E_{rec}. The recuperation energy involves two flow ways (i.e., the input and output ways), as shown in Fig. 5. The recuperation capability is governed by the loss of each step, the motor torque limitation, and the lithium-ion battery current and charge limitations.

Firstly, we find the time set S such that

$$S = \{t | t \in [t_0, t_f], P(t) - P_{au}(t) < 0, \boldsymbol{P_b}(t) < 0\}. \tag{20}$$

Note that the auxiliary power demand P_{au} is physically loaded at the converter. The absolute input energy for the set S at the wheels per distance, $E_{w,in}$, is calculated by

$$E_{w,in} = \frac{\int_S |P(t) - P_{au}(t)|dt}{d}. \tag{21}$$

The associated net energy stored in the battery

$$E_{b,in} = \frac{\int_S |P_b(t) + I(t)^2 R n_c|dt}{d}. \tag{22}$$

The resulting energy loss

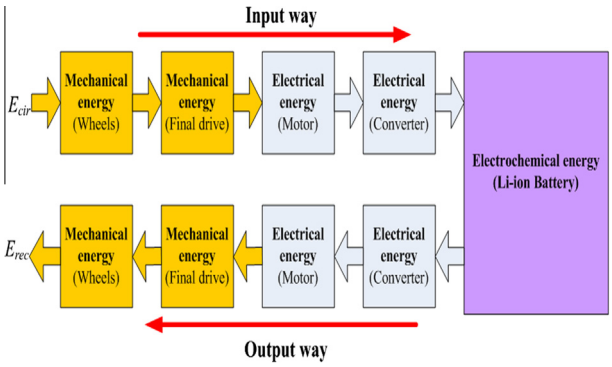

Fig. 5. Schematic of recuperation energy flow of the bus.

$$E_{loss,in} = E_{w,in} - E_{b,in} - \frac{\int_S P_{au}(t)dt}{d}. \quad (23)$$

The cycle-averaged wheel-to-battery energy efficiency can thus be obtained by

$$\eta_{wb,in} = 1 - \frac{E_{loss,in}}{E_{w,in}}, \quad (24)$$

yielding the net recuperation energy stored in the battery

$$E_{rec,in} = E_{cir}\eta_{wb,in}. \quad (25)$$

Then, we find the time set D such that

$$D = \{t | t \in [t_0, t_f], P(t) - P_{au}(t) \geq 0, \boldsymbol{P_b}(t) \geq 0\}. \quad (26)$$

The associated motor energy loss in propelling condition

$$E_{loss,m} = \frac{\int_D P_{loss,m}(t)dt}{d}, \quad (27)$$

and the averaged motor efficiency is

$$\eta_{m,out} = 1 - \frac{E_{loss,m}d}{\int_D \boldsymbol{P_b}}(t)\eta_{con} + \boldsymbol{P_{egu}}(t)\eta_{con} - P_{au}(t)dt. \quad (28)$$

The battery energy loss in the time set D

$$E_{loss,b} = \frac{\int_D I(t)^2 R n_b dt}{d}, \quad (29)$$

and the corresponding battery efficiency in the output way is

$$\eta_{b,out} = 1 - \frac{E_{loss,b}d}{\int_D P_b(t) + I(t)^2 R n_b dt}. \quad (30)$$

The cycle-averaged battery-to-wheel energy efficiency can thus be obtained by

$$\eta_{bw,out} = \eta_{b,out}\eta_{con}\eta_{m,out}\eta_{fd}, \quad (31)$$

where η_{fd} is the efficiency of the final drive. According to Eqs. (25) and (31), we can acquire the net recuperation energy for traction

$$E_{rec} = E_{rec,in}\eta_{bw,out}, \quad (32)$$

and the cycle-averaged recuperation efficiency

$$\eta_{rec} = \frac{E_{rec}}{E_{cir}} = \eta_{wb,in}\eta_{bw,out}. \quad (33)$$

3.3. Fuel-to-traction efficiency

The fuel-to-traction efficiency is defined as

$$\eta_{ft} = \frac{E_{trac}}{E_{ef}} = \frac{E_{dis} + (1 - \eta_{rec})E_{cir}}{E_{ef}}, \quad (34)$$

where E_{ef}, termed as the equivalent fuel energy, is the sum of the consumed diesel energy and electric energy per distance. η_{ft} is the cycle-averaged conversion efficiency from the total consumed energy (diesel and electricity) to the mechanical energy at the wheels and the electrical energy for the auxiliaries. Compared to the electrical and mechanical paths, the ICE has a far lower efficiency, leading to the dominant restriction for η_{ft}. Given Eq. (34), the equivalent fuel energy E_{ef} is obtained by

$$E_{ef} = \frac{E_{dis} + (1 - \eta_{rec})E_{cir}}{\eta_{ft}}. \quad (35)$$

Then, based on the initial and final values of the battery SOC, E_{ef} can be simply split to achieve the individual diesel energy and electricity.

4. Energy management strategies based on convex optimization

4.1. Convex modeling

A convex optimization problem can be written as follows:

$$\begin{array}{ll} \text{minimize} & f_0(\boldsymbol{x}) \\ \text{subject to} & f_i(\boldsymbol{x}) \leqslant 0, \quad i = 1, \ldots, m \\ & h_j(\boldsymbol{x}) = 0, \quad j = 1, \ldots, p \\ & \boldsymbol{x} \in \boldsymbol{\chi}, \end{array} \quad (36)$$

where $\boldsymbol{\chi} \in \mathbb{R}^n$ is a convex set, $f_i(\boldsymbol{x}), i = 0, \ldots, m$, are convex functions, and $h_j(x)$ are affine functions in the optimization vector $\boldsymbol{x}$ [33]. In our studied problem, the optimization variables are $\boldsymbol{T}(t)$, $\boldsymbol{P_b}(t)$, $\boldsymbol{P_{egu}}(t)$, and $\boldsymbol{SOC}(t)$, and the constraints are vehicle power balance, i.e., Eq. (5), and the battery constraints Eqs. (9)–(13). It is easy to notice that Eqs. 5, 9, and 10 do not comply with the definition of a convex problem. Eq. (5) can be written as convex, by relaxing the equality to inequality; it has been suggested in [34] that Eqs. (9) and (10) can be reformulated as convex functions by introducing a new variable

$$\boldsymbol{E}(t) = \frac{CV_{oc}^2(t)n}{2} \quad (37)$$

with $C = \frac{2Q_n}{\bar{V}_{oc}}$. The resulting convex constraints are then given as

$$P_m(t) + P_{loss,m}(t) + P_{au}(t) \leqslant \min\left(\boldsymbol{P_b}(t)\eta_{con}, \frac{\boldsymbol{P_b}(t)}{\eta_{con}}\right) + \boldsymbol{P_{egu}}(t)\eta_{con}, \quad (38)$$

$$\boldsymbol{P_b}(t) \geqslant \sqrt{\frac{2\boldsymbol{E}(t)n_c}{C}}I_{\min} - RI_{\min}^2 n_c, \quad (39)$$

$$\boldsymbol{P_b}(t) \leqslant \frac{\boldsymbol{E}(t)}{2RC}, \quad (40)$$

$$\boldsymbol{E}(t) - \sqrt{\boldsymbol{E}^2(t) - 2RC\boldsymbol{E}(t)\boldsymbol{P_b}(t)} \leqslant I_{\max}R\sqrt{2CE(t)n_c}, \quad (41)$$

$$\frac{d\boldsymbol{E}(t)}{dt} \leqslant -\frac{d_0}{RQ_n}(\boldsymbol{E}(t) - \sqrt{\boldsymbol{E}^2(t) - 2\boldsymbol{R}CE(t)\boldsymbol{P_b}(t)}), \quad (42)$$

$$\boldsymbol{E}(t) \in \frac{C}{2}[V_{oc}^2(SOC_{\min}), V_{oc}^2(SOC_{\max})]n_c, \quad (43)$$

$$\boldsymbol{E}(t_0) = \frac{C}{2}V_{oc}^2(SOC_0)n_c. \quad (44)$$

4.2. Energy management strategies

As opposed to HEVs, the battery charge in PHEVs is used. The optimal energy control strategy for PHEVs is often defined to minimize the equivalent fuel cost (i.e., liquid fuel and electricity). For trips shorter than the all electric range (AER), PHEVs are equivalent to battery electric vehicles (BEVs), and the associated optimal energy control-charge depleting (CD) mode-is deployed, since electricity is considerably cheaper than liquid fuel [35]. The optimal strategy in this case is trivial [35–37]. The discussed plug-in hybrid electric bus has a fixed driving route longer than the AER, which gives a degree of freedom concerning the optimal power split between the battery and the EGU. Otherwise, it will become a battery electric bus that typically needs considerably larger and more expensive battery pack. Two feasible energy management strategies, based on convex optimization, are considered. One is the CD–CS strategy for which the bus firstly operates in CD mode until the battery charge arrives at a pre-specified threshold and then switches to convex-optimization-based CS mode; the other is the blended strategy, implying that the optimal power allocation between the battery and the EGU is attained throughout the route by convex optimization. The two strategies are formulated in Table 3. In order to guarantee a fair comparison, the final battery SOC for the two strategies should be identical. The natural and straightforward form of the convex optimization problem is automatically parsed by a tool, CVX [33,38], so as to derive a general

Table 3
Two energy management strategies for the plug-in bus.

Convex-optimization-based energy management
1. CD–CS strategy (1) CD Phase (no optimization) For $k = 1, \ldots, N_{cd}$, with $SOC(N_{cd}+1)$ corresponding to the switching SOC (25% in our case) (a) Solve the cell current $I_0(k)$ algebraically, according to the calculated battery power $P_{b,0}$ without considering the cell current and charge limitations: $T_{(k)} \in [T_{min}(\omega(k)), T_{max}(\omega(k))]$, $P_m(t) + P_{loss,m}(t) + P_{au}(t) = \min\left(P_{b,0}(t)\eta_{con}, \frac{P_{b,0}(t)}{\eta_{con}}\right)$, $I_0(k) = \frac{V_{oc}(k) - \sqrt{V_{oc}^2(k) - \frac{4P_{b,0}(k)}{n_c R}}}{2R}$. (b) Achieve the correct cell current $I(k)$, considering the cell current and charge limitations: $I(k) \in [I_{min}, I_{max}]$, $SOC(k+1) = SOC(k) - \frac{I(k)\Delta t}{Q_n}$, $SOC(k) \in [SOC_{min}, SOC_{max}]$. Δt is the time interval.) (c) Calculate the correct battery power $P_b(k) = V_{oc}(k)I(k)n_c - I^2(k)Rn_c$, $SOC(k)$, $E(k)$, and $T(k)$. Note that the above limitations are only active when the friction braking is needed. (2) CS Phase (convex optimization) For $k = N_{cd}+1, \ldots, N$, with N corresponding to the final time step Variables: $P_b(N-N_{cd})$, $P_{egu}(N-N_{cd})$, $E(N+1-N_{cd})$, $T(N-N_{cd})$ (the number in parentheses is the vector length) Expressions: $P_f(N-N_{cd})$, $P_m(N-N_{cd})$, $P_{loss,m}(N-N_{cd})$, $J_c = \sum_{k=N_{cd}+1}^{N} c_f P_f(k)\Delta t$ Minimize J_c Subject to Eqs. (38)–(43), $E(N_{cd}+1) = E(N+1)$, $T(k) \in [T_{min}(\omega(k)), T_{max}(\omega(k))]$, $P_{egu}(k) \in [0, P_{max,egu}]$, $P_{egu}(e_{off}) = 0$ (e_{off} is an index vector of $e(k) = 0$, indicating the engine-off steps.) 2. Blended strategy (convex optimization) For $k = 1, \ldots, N$, with N corresponding to the final time step Variables: $P_b(N)$, $P_{egu}(N)$, $E(N+1)$, $T(N)$ Expressions: $P_f(N)$, $P_m(N)$, $P_{loss,m}(N)$, $J_c = \sum_{k=1}^{N} c_f P_f(k)\Delta t + c_{el}(SOC_0 - SOC_f)Q_n\overline{V}_{oc}n_c$ Minimize J_c Subject to Eqs. (38)–(44), $E(N+1) = \frac{c}{2}V_{oc}^2(SOC_f)n_c$, $T(k) \in [T_{min}(\omega(k)), T_{max}(\omega(k))]$, $P_{egu}(k) \in [0, P_{max,egu}]$, $P_{egu}(e_{off}) = 0$

semi-definite program (SDP) form. The bold variables are parameters to optimize (see Section 4.1). Note that the so-called expressions in the table are not equality constraints, but are merely used for better readability. CVX substitutes the expressions with the corresponding mathematical operations. After these, the problem is passed to the solver, SeDuMi [39,40], to obtain the optimal variables with high computational efficiency. Since the optimization problem is convex, instead of trapping into local minima, a global optimization solution can be rapidly accomplished, with any initialization. Please refer to [33] to find more details on the theoretical and algorithmic properties of convex optimization.

5. Results and discussion

5.1. Efficiency analysis and comparison of the two energy control algorithms

Given the driving cycle and the optimal variables extracted by the foregoing algorithms, the recuperation and fuel-to-traction efficiencies can be calculated, as Section 3 describes. Before discussing the two efficiencies, it is important to investigate the operating states of the power sources (the battery and the EGU) in the powertrain. The cell SOC and current distribution for the two strategies are shown in Fig. 6. It is clear that both the average and maximum absolute cell currents in the blended algorithm are smaller than those in the CD–CS algorithm, leading to less battery energy loss. Observing the SOC trajectory, we can further conclude that the current difference is mainly existent in the discharging process. The round-trip battery efficiency and the recuperation efficiencies in the input and output directions are shown in Fig. 7. Compared to the CD–CS strategy, the blended scenario has obviously higher averaged battery efficiency (by 1.73%) and recuperation efficiency in the output way (by 1.32%), because of much smaller discharging current. A slightly better recuperation efficiency in the input way is also observed for the blended algorithm, because cells have a slightly higher OCV (see Figs. 4 and 6) during charging and thus a little smaller energy loss, given the same charging power. The EGU efficiencies for the two strategies are similar, as shown in

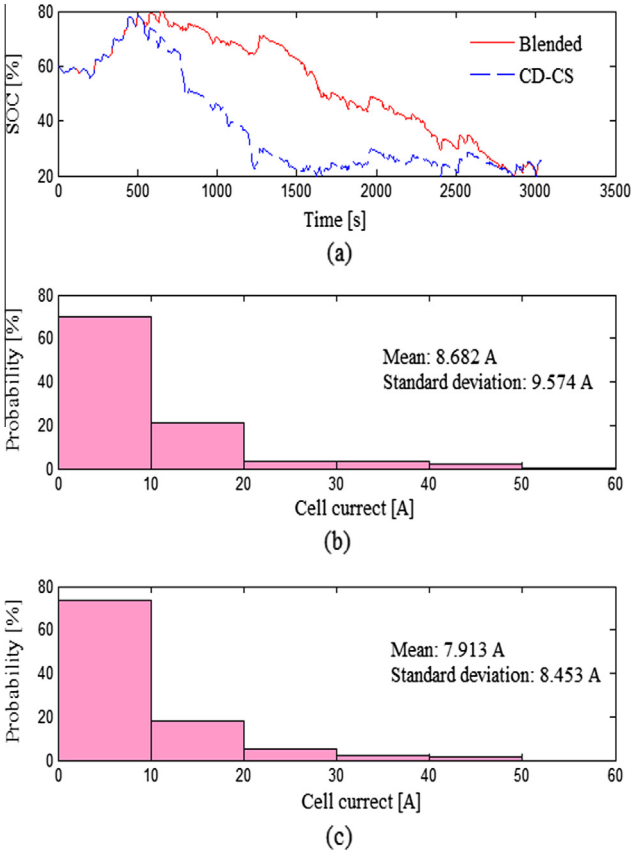

Fig. 6. (a) SOC trajectories, (b) absolute current distribution in the CD–CS strategy, and (c) absolute current distribution in the blended strategy.

Fig. 8, since the convex optimization is used to determine the optimal EGU power in both strategies. The recuperation efficiency, fuel-to-traction efficiency, and energy consumption per kilometer are shown in Fig. 9. The recuperation efficiency for the CD–CS

strategy is 64.86%, while that for the blended strategy is 66.13% – an improvement of 1.27% mainly resulting from the battery current deviation. The fuel-to-traction efficiency for the CD–CS strategy is 35.83%, while that for the blended strategy is 36.13%-an improvement of 0.3%. The fuel-to-traction efficiency is mainly limited by the EGU efficiency (see Fig. 8) and also affected by energy losses occurring in other electrical and mechanical paths, e.g., battery, power converter, electric motor, and final drive. The energy consumption per kilometer for the CD–CS strategy is 9.02 MJ, while that for the blended strategy is 8.87 MJ – an improvement of 0.15 MJ. Since both strategies consume the same amount of electricity, the blended strategy can save diesel energy of 0.15 MJ per kilometer, which is attributed to the superior recuperation and fuel-to-traction efficiencies. It is worth mentioning that since the transit bus runs approximately 50,000 km per year (much longer than standard passenger cars), the energy saving caused by the more advanced blended strategy is significant.

5.2. Impact of battery downsizing on the bus energy efficiency

In addition to a better TTW energy conversion, Section 5.1 shows that the blended energy control algorithm needs less battery discharging power, inducing a potential of reducing the battery size. As lithium-ion battery is still highly costly in the market and is the most expensive component in the bus powertrain, downsizing is of great significance for decreasing the purchase cost of the bus. However, it is necessary to assess the influence of battery downsizing on the recuperation and fuel-to-traction efficiencies of the plug-in bus. Given the reduced battery sizes, the round-trip battery efficiency and the recuperation efficiencies in the input and output directions are shown for the optimal blended strategy in Fig. 10. It is notable that all the three efficiencies become lower with the battery downsizing. In particular, the recuperation efficiency in the input way has a dramatic

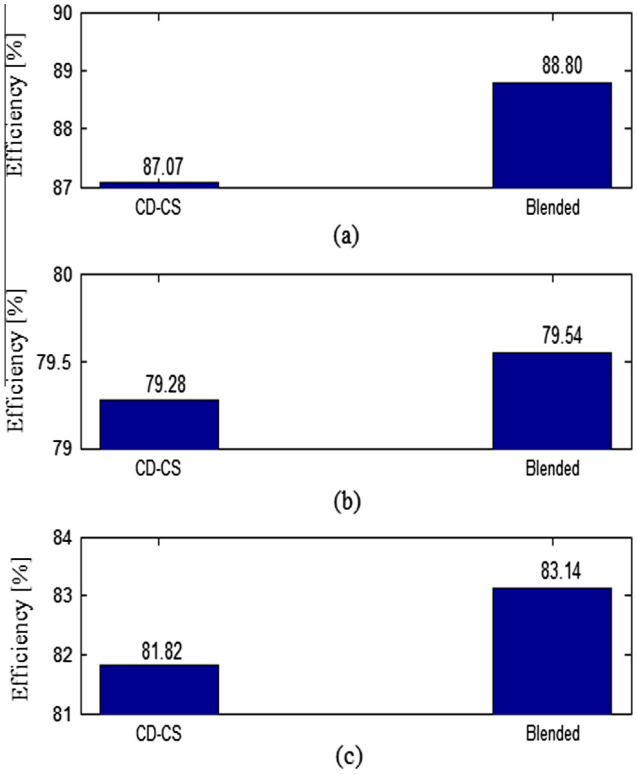

Fig. 7. (a) Round-trip battery efficiency, (b) recuperation efficiency in the input way, and (c) recuperation efficiency in the output way.

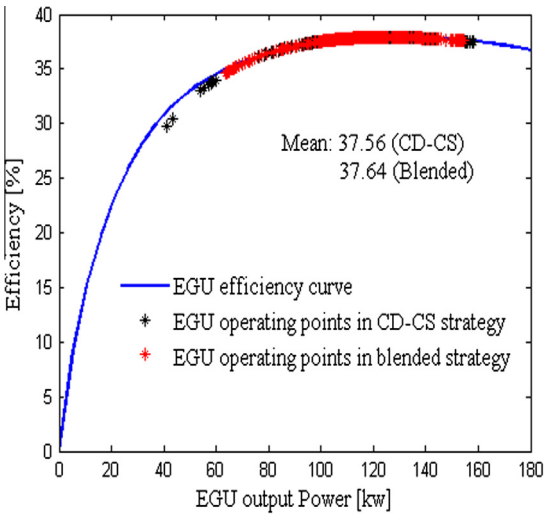

Fig. 8. EGU efficiencies.

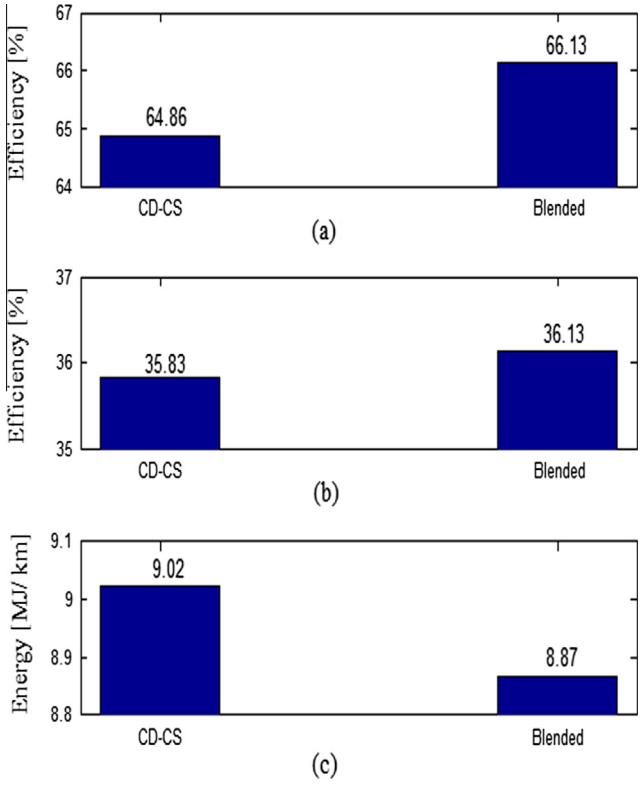

Fig. 9. (a) Recuperation efficiency (two-way), (b) fuel-to-traction efficiency, and (c) energy consumption per distance.

drop, since the battery current has an evident increase during recuperation when the engine is off, and the friction braking is more likely to be used to meet the current and charge limitations.

The associated impact on the recuperation efficiency, fuel-to-traction efficiency, and energy consumption per kilometer are shown in Fig. 11. It can be found that the battery downsizing has an apparently negative effect on the recuperation efficiency of the bus. The fuel-to-traction efficiency also decreases with the reduced battery size. Owing to the deterioration of the two efficiencies, the energy consumption per kilometer increases. Therefore, there is a tradeoff between battery downsizing and energy efficiency. The battery should be downsized with a careful consider-

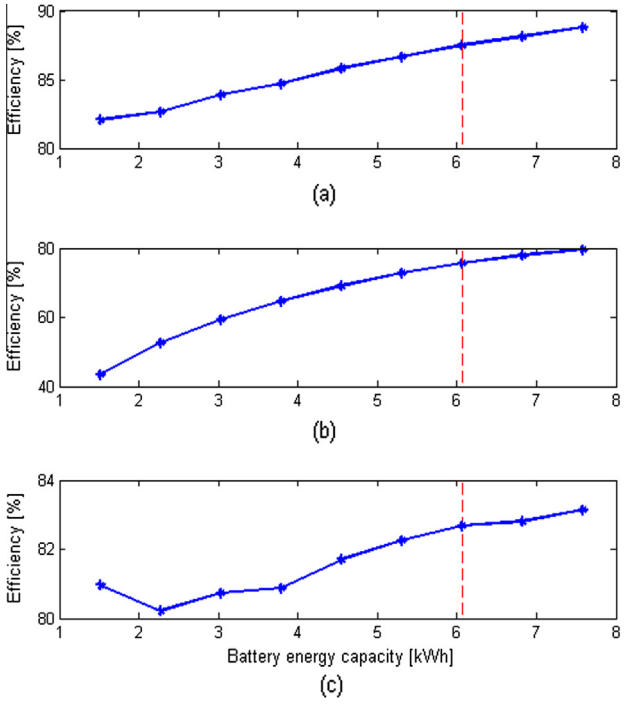

Fig. 10. Efficiency versus battery size: (a) round-trip battery efficiency; (b) recuperation efficiency in the input way; (c) recuperation efficiency in the output way.

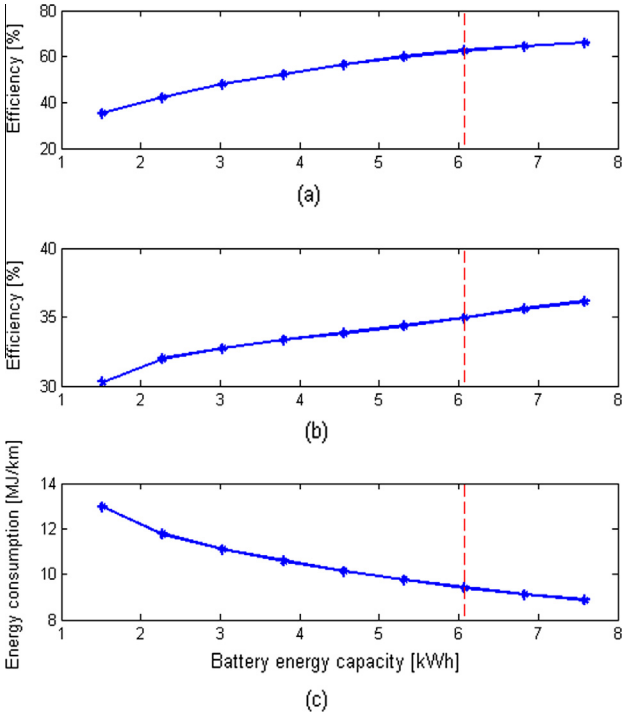

Fig. 11. Efficiency versus battery size: (a) recuperation efficiency (two-way); (b) fuel-to-traction efficiency; (c) energy consumption per distance.

ation without sacrificing the two efficiencies to an unacceptable degree. For example, if the recuperation and fuel-to-traction efficiencies are required not to be less than 63% and 35%, respectively, there will be a possibility of reducing the pack by 1.52 kW h. On the other hand, from a viewpoint of cost, the tradeoff is between the purchase cost and the operating cost, and the total ownership cost (TCO) should thus be considered. However, it is not trivial to find the best solution, since TCO depends on a variety of factors, such as diesel price, electricity price, battery price, total bus mileage, and battery replacement.

6. Conclusions

This paper analyzes the TTW energy conversion efficiency of a series plug-in hybrid electric bus operating in Gothenburg, Sweden. The TTW process is characterized by the recuperation and fuel-to-traction efficiencies, which are quantified and compared for two optimization-based energy management strategies, i.e., the CD–CS and blended energy controls. The convex modeling of the bus powertrain is performed, and the efficient convex optimization is used for the two strategies. The efficiency analysis indicates that the recuperation efficiencies for the CD–CS and blended strategies are 64.86% and 66.13%, respectively; the fuel-to-traction efficiencies are 35.83% and 36.13%; the diesel energy consumptions per kilometer are 9.02 MJ and 8.87 MJ. The blended algorithm thus leads to a more efficient TTW energy conversion of the plug-in bus. Considering the potential of downsizing the battery for the blended algorithm that requires less battery discharging power, we also quantify the impact of battery downsizing on the recuperation and fuel-to-traction efficiencies and the energy consumption per kilometer. It can be found that as the battery energy capacity decreases, the two efficiencies become worse. There is, therefore, a tradeoff between the battery downsizing and energy efficiencies for the plug-in bus with the blended energy management strategy.

Acknowledgement

This work was supported by Swedish Energy Agency.

References

[1] Juul N, Meibom P. Road transport and power system scenarios for Northern Europe in 2030. Appl Energy 2012;92:573–82.
[2] Takeshita T. Assessing the co-benefits of CO_2 mitigation on air pollutants emissions from road vehicles. Appl Energy 2012;97:225–37.
[3] Kudoh Y, Ishitani H, Matsuhashi R, Yoshida Y, Morita K, Katsuki S, et al. Environmental evaluation of introducing electric vehicles using a dynamic traffic-flow model. Appl Energy 2001;69:145–59.
[4] Ehsani M, Gao Y, Gay SE, Emadi A. Modern electric, hybrid electric, and fuel cell vehicles-fundamentals, theory, and design. Boca Raton: CRC Press; 2005.
[5] Guzzella L, Sciarretta A. Vehicle propulsion systems-introduction to modeling and optimization. 2nd ed. Berlin: Springer; 2007.
[6] Mi C, Masrur MA, Gao DW. Hybrid electric vehicles-principles and applications with practical perspectives. West Sussex: John Wiley & Sons; 2011.
[7] Zhang X, Mi C. Vehicle power management-modeling, control and optimization. Berlin: Springer; 2011.
[8] Sheu KB. Simulation for the analysis of a hybrid electric scooter powertrain. Appl Energy 2008;85:589–606.
[9] Doucette RT, McCulloch MD. Modeling the prospects of plug-in hybrid electric vehicles to reduce CO_2 emissions. Appl Energy 2011;88:2315–23.
[10] Samaras C, Meisterling K. Life cycle assessment of greenhouse gas emissions from plug-in hybrid vehicles: implications for policy. Environ Sci Technol 2008;42:3170–6.
[11] Demirdöven N, Deutch J. Hybrid cars now, fuel cell cars later. Science 2004;305:974–6.
[12] Guzzella L. Automobiles of the future and the role of automatic control in those systems. Annu Rev Control 2009;33:1–10.
[13] Williamson SS, Emadi A. Comparative assessment of hybrid electric and fuel cell vehicles based on comprehensive well-to-wheels efficiency analysis. IEEE Trans Vehicle Technol 2005;54:856–62.
[14] Hawkins TR, Gausen OM, Strømman AH. Environmental impacts of hybrid and electric vehicles – a review. Int J Life Cycle Assess 2012;17:997–1014.
[15] Ahman M. Primary energy efficiency of alternative powertrains in vehicles. Energy 2000;26:973–89.
[16] Ott T, Zurbriggen F, Onder C, Guzzella L. Cycle-averaged efficiency of hybrid electric vehicles. Proc Inst Mech Eng Pt D J Automob Eng 2013;227:78–86.

[17] Katrašnik T, Trenc F, Opresnik SR. Analysis of energy conversion efficiency in parallel and series hybrid powertrains. IEEE Trans Vehicle Technol 2007;56:3649–59.
[18] Katrašnik T. Analytical framework for analyzing the energy conversion efficiency of different hybrid electric vehicle topologies. Energy Convers Manage 2009;50:1924–38.
[19] Katrašnik T. Energy conversion efficiency of hybrid electric heavy-duty vehicles operating according to diverse drive cycles. Energy Convers Manage 2009;50:2865–78.
[20] Katrašnik T. Analytical method to evaluate fuel consumption of hybrid electric vehicles at balanced energy content of the electric storage devices. Appl Energy 2010;87:3330–9.
[21] Katrašnik T. Energy conversion phenomena in plug-in hybrid-electric vehicles. Energy Convers Manage 2011;52:2637–50.
[22] Kum D, Peng H, Bucknor NK. Optimal control of plug-in HEVs for fuel economy under various travel distances. In: Proceedings of the 6th IFAC symposium advances in automotive control, Munich, Germany, 12–14 July; 2010. p. 258–63.
[23] Moura SJ, Fathy HK, Callaway DS, Stein JL. A stochastic optimal control approach for power management in plug-in hybrid electric vehicles. IEEE Trans Control Syst Technol 2011;19:545–55.
[24] Keefe MPO, Markel T. Dynamic programming applied to investigate energy management strategies for a plug-in HEV. In: Proceedings of the 22nd international battery, hybrid and fuel cell electric vehicle, Yokohama, Japan, 23–28 October; 2006.
[25] Tulpule P, Marano V, Rizzoni G. Energy management for plug-in hybrid electric vehicles using equivalent consumption minimisation strategy. Int J Electric Hybrid Vehicle 2010;2:329–50.
[26] Stockar S, Marano V, Canova M, Rizzoni G, Guzzella L. Energy-optimal control of plug-in hybrid electric vehicles for real-world driving cycles. IEEE Tran Vehicle Technol 2011;60:2949–62.
[27] Zhang C, Vahidi A. Route preview in energy management of plug-in hybrid vehicles. IEEE Trans Control Syst Technol 2012;20:546–53.
[28] Xu L, Ouyang M, Li J, Yang F, Lu L, Hua J. Optimal sizing of plug-in fuel cell electric vehicles using models of vehicle performance and system cost. Appl Energy 2013;103:477–87.
[29] Murgovski N, Johannesson L, Sjöberg J, Egardt B. Component sizing of a plug-in hybrid electric powertrain via convex optimization. Mechatronics 2012;22:106–20.
[30] Murgovski N, Johannesson L, Hellgren J, Egardt B, Sjöberg J. Convex optimization of charging infrastructure design and component sizing of a plug-in series HEV powertrain. In: Proceedings of the 18th IFAC World Congress, Milano, Italy, 28 August – 2 September; 2011. p. 13052–7.
[31] Pourabdollah M, Murgovski N, Grauers A, Egardt B. Optimal sizing of a parallel PHEV powertrain. IEEE Trans Vehicle Technol 2013;62:2469–80.
[32] Gaines L, Cuenca R. Costs of lithium-ion batteries for vehicles. Technical report 2000, Center for Transportation Research at Argonne National Laboratory, US Department of Energy.
[33] Boyd S, Vandenberghe L. Convex optimization. Cambridge: Cambridge University Press; 2004.
[34] Murgovski N, Johannesson L, Sjöberg J. Convex modeling of energy buffers in power control applications. In: Proceedings of IFAC workshop on engine and powertrain control, simulation and modeling, Paris, France, 23–25 October; 2012.
[35] Larsson V, Johannesson L, Egardt B. Impact of trip length uncertainty on optimal discharging stategies for PHEVs. In: Proceedings of the 6th IFAC Symposium Advances in Automotive Control, Munich, Germany, 12–14 July, 2010; 55–60.
[36] Larsson V, Johannesson L, Egardt B, Lassson A. Benefit of route recognition in energy management of plug-in hybrid electric vehicles. In: Proceedings of American control conference, Montreal, Canada, 27–29 June; 2012. p. 1314–20.
[37] Pourabdollah M, Larsson V, Johannesson L, Egardt B. PHEV energy management: a comparison of two levels of trip information. SAE Technical paper 2012-01-0745, SAE World Congress & Exhibition, Detroit, USA, 24–26 April, 2012.
[38] Grant M, Boyd S. CVX: Matlab software for disciplined convex programming, version 1.21. <http://cvxr.com/cvx> (May 2010).
[39] Labit Y, Peaucelle D, Henrion D. SeDuMi interface 1.02: a tool for solving LMI problems with SeDuMi. In: Proceedings of IEEE international symposium on computer aided control system design, Glasgow, Scotland, UK, 18–20 September; 2002. p. 272–7.
[40] Murgovski N. Optimal powertrain dimensioning and potential assessment of hybrid electric vehicles. PhD dissertation, Chalmers University of Technology, Gothenburg, Sweden, 2012.